International Journal of Management, Finance and Accounting

Sectoral Shockwaves: Examining Bursa Malaysia's Sector Indices Amid the COVID-19 Pandemic

Alyssa April Dellow[1], Hafizah Bahaludin[2,*]

[1]Department of Mathematical Sciences, Faculty of Science and Technology, Universiti Kebangsaan Malaysia, Selangor, Malaysia
[2]Department of Computational and Theoretical Sciences, Kulliyyah of Science, International Islamic University Malaysia, Pahang, Malaysia
*Corresponding author: hafizahbahaludin@iium.edu.my
(ORCiD: 0000-0002-6364-9638)

Abstract

The Coronavirus disease 2019 (COVID-19) outbreak is becoming a widespread concern, as it is causing a decline in economies and negatively impacting stock markets worldwide. As the Malaysian government implements the Movement Control Order (MCO) to curb the spread of the deadly virus, the Malaysian stock market is rapidly impacted, becoming volatile and unpredictable throughout the pandemic phase. Thus, this study aims to analyse the structural correlation patterns of the Bursa Malaysia Sectoral Index Series using the threshold network approach. The data utilised in this study are the closing prices of all 13 sectoral indexes, spanning from January 1, 2019, to December 31, 2021. Threshold networks are constructed for the years 2019, 2020, and 2021 based on different threshold values to visualise the correlation between indexes. The results suggested that COVID-19 affected the Malaysian stock market, as the indexes appeared to be more correlated with each other in 2020. In addition, consumer products and services (KLCM), industrial products and services (KLIP), property (KLPR), and construction (KLCT) emerged as the most influential indexes throughout the pandemic. This study will help market participants gain an understanding of the correlation between indexes based on threshold networks.

This work is licensed under the Creative Commons BY-NC-ND 4.0 International License.
© University Telekom Sdn. Bhd.
Published by MMU PRESS. URL https://journals.mmupress.com/ijomfa

Keywords: COVID-19, Cross-Correlation, Threshold Network, Bursa Malaysia, Centrality Measures

Received on 9 April 2025; Accepted on 14 June 2025; Published on 28 February 2026

To cite this article: Dellow, A. A., & Bahaludin, H. (2026). Sectoral shockwaves: Examining Bursa Malaysia's sector indices amid the COVID-19 pandemic. *International Journal of Management, Finance and Accounting*, *7*(1), 84-121. https://doi.org/10.33093/ijomfa.2026.7.1.4

1.0 Introduction

The global outbreak of COVID-19 declared a pandemic by the World Health Organisation (WHO), has had far-reaching implications for public health, economic activity, and financial systems worldwide. As of July 1, 2022, over 545 million confirmed cases and more than 6.3 million deaths have been reported globally (World Health Organization, 2022). Malaysia accounted for over 4.5 million confirmed cases and nearly 36,000 deaths, representing 0.84% of global infections. The first case in Malaysia was reported on January 25 2020, with a surge in cases during March following the Sri Petaling tabligh cluster (Sheikh Yahya, 2020). In an urgent response to contain the outbreak, the Malaysian government implemented a nationwide Movement Control Order (MCO) on March 18 2020, invoking the Prevention and Control of Infectious Diseases Act 1988 and the Police Act 1967. The MCO entailed restrictions on mass gatherings, the closure of non-essential businesses, and bans on interstate travel (14-Day Movement Control Order Begins, 2020). These containment measures brought much of the economy to a standstill, profoundly impacting the financial markets.

The pandemic led to a significant downturn in Bursa Malaysia, as reflected by the performance of the FTSE Bursa Malaysia KLCI (FBM KLCI). The index plummeted to historic lows in March 2020 as investors responded to heightened uncertainty and deteriorating economic forecasts (Amir et al., 2022; Song et al., 2021). Although partial recovery followed the announcement of fiscal support and vaccination rollouts, volatility persisted through 2021, illustrating the fragile state of investor sentiment (Sah & Wong, 2021; Liew et al., 2022). While the FBM KLCI illustrates the overall market trajectory, a closer look at individual sectoral indices reveals a more nuanced picture. COVID-19 did not affect all sectors equally. According to a study by Lee et al. (2020), all 13 major sectoral indices in Bursa Malaysia experienced negative performance during the initial outbreak, except for the Plantation Index, which remained relatively resilient. This suggests a level of sector-specific immunity, possibly due to the Plantation sector's exposure to global commodity demand and its role in essential supply chains.

Financial services and real estate investment trusts (REITs), for example, initially benefited from policy signals related to interest rate cuts and liquidity support. However, these gains were short-lived as the prolonged nature of the pandemic led to loan moratoriums, delayed rental payments, and weaker commercial activity (Chow & Tan, 2022; Chee et al., 2024). The Construction, Energy, and Utilities sectors, typically more sensitive to long-term government projects and consumption patterns, showed moderate to minimal reactions, suggesting a lagged or dampened effect during the initial phases of the crisis (Chee et al., 2024).

On the other hand, smaller-cap stocks, which are often more nimble and domestically focused, experienced periods of outperformance, especially when stimulus packages were implemented. Liew et al. (2022) reported that these firms, less encumbered by international exposure and large-scale capital structures, were more responsive to local government support, making them attractive during uncertain times. Similar asymmetric impacts have been documented in other markets. For instance, Estrada et al. (2020) found that sectors such as tourism, international trade, and transportation in China were severely hit, while electricity consumption increased dramatically due to lockdown-induced demand from households and medical institutions. Likewise, Li et al. (2020) and Tashanova et al. (2020) highlighted the bullish performance of the healthcare and biotech sectors, positioning them as safe-haven investments during the pandemic.

The pandemic also altered how sectors interacted within the stock market. Increased correlations and shifts in systemic importance among sectoral indices were observed, suggesting changes in the underlying market structure. Aslam et al. (2020) and Zhang et al. (2020) documented heightened co-movement among global stock markets, revealing a contraction of diversification benefits during crisis periods. To analyse such dynamics within Bursa Malaysia, complex network theory offers a powerful lens. Mantegna (1999) pioneered the use of correlation-based Minimum Spanning Trees (MSTs) to understand hierarchical relationships among stocks. This method was extended by Tumminello et al. (2005) into the Planar Maximally Filtered Graph (PMFG), which preserves more information while maintaining a hierarchical structure. However, both methods impose topological constraints that may lack economic justification (Výrost et al., 2015).

In contrast, the threshold network method allows greater flexibility. Edges are retained only if correlation values exceed a statistically determined threshold (Boginski et al., 2004). This method has been proven effective in crisis settings, as demonstrated in studies by Li and Pi (2018), Nobi et al. (2014), and Xia et al. (2018). Given its adaptability and interpretability, this study employs the threshold network approach to examine the dynamic structural changes among Bursa Malaysia's sectoral indices from 2019 to 2021. This study contributes to the growing body of literature on financial networks and pandemic-induced market stress. While previous studies often focused on global indices or selected market segments, this research provides a comprehensive analysis of all 13 sectoral indices in Bursa Malaysia using threshold network models. Furthermore, the study applies centrality measures that include degree, closeness, betweenness, and eigenvector (Freeman, 1977; Bonacich, 1987). The centrality measures are employed to identify influential sectors over time, revealing structural shifts in market leadership during the COVID-19 pandemic.

The objectives of this study are outlined as follows:

1. To analyse the structural correlation patterns among Bursa Malaysia's 13 sectoral indices from 2019 to 2021.

2. To construct threshold-based networks using correlation matrices and investigate their topological properties over time.

3. To identify dominant sectoral indices based on multiple centrality measures (degree, closeness, betweenness, eigenvector).

The remainder of this paper is structured as follows. Section 2 discusses the data utilised in this study, besides preparing an elaborate explanation on the methodology of the cross-correlation-based threshold network approach and centrality measures. Section 3 presents and discusses the results of the analysis carried out. Lastly, concluding remarks can be found in Section 4.

2.0 Data

In this study, all 13 Bursa Malaysia sectorial indexes are utilised to construct threshold networks. As part of the Bursa Malaysia Sectorial Index Series, each index tracks the performance of companies listed on the Main Market, categorised by their respective sectors. The daily closing price data for each of the 13 indexes from January 1, 2019, to December 31, 2021, is downloaded from Refinitiv Eikon. The period under study comprises 737 trading days, which are further divided into three subperiods to be investigated through network analysis, enabling the study of these networks' topological properties over time. These three timelines cover 244 trading days in 2019 (January 1, 2019, to December 31, 2019), 248 trading days in 2020 (January 1, 2020, to December 31, 2020), and 245 trading days in 2021 (January 1, 2021, to December 31, 2021). RStudio is used for the entirety of the analyses carried out. Table 1 displays all 13 index names along with their tickers that are used throughout this study.

Table 1: List of Indexes and their Tickers

No	Ticker	Index Name
1	KLCT	Construction
2	KLCM	Consumer Products and Services
3	KLEN	Energy
4	KLFI	Financial Services
5	KLHC	Health Care
6	KLIP	Industrial Products and Services
7	KLPL	Plantation
8	KLPR	Property
9	KLRE	Real Estate Investment Trusts (REIT)
10	KLTE	Technology
11	KLTC	Telecommunications and Media
12	KLTP	Transportation and Logistics
13	KLUT	Utilities

3.0 Methodology

This subsection emphasises the cross-correlation-based threshold network approach and centrality measures. To assess the impact of COVID-19 on the Malaysian stock market, the threshold networks for 2019, 2020, and 2021, along with their centrality measures, are obtained to facilitate comparisons.

3.1 Rate of Return

The first step in a series of standard procedures to construct a stock market network, or in this study, a sectorial index network, is to calculate the logarithmic returns of the indexes as follows:

$$r_i(t) = \ln\left[\frac{P_i(t)}{P_i(t-1)}\right], \tag{1}$$

where $P_i(t)$ is the closing price and $r_i(t)$ is the logarithmic return of index i on day t.

3.2 Cross-Correlation

Given that there are N indexes, the correlations between all pairs of indexes are obtained from a $N \times N$ Pearson correlation matrix computed in R. The Pearson correlation coefficient (Mantegna, 1999) among any two indexes from the matrix can be computed as shown below:

$$C_{ij} = \frac{\langle r_i r_j \rangle - \langle r_i \rangle \langle r_j \rangle}{\sqrt{\left(\langle r_i^2 \rangle - \langle r_i \rangle^2\right)\left(\langle r_j^2 \rangle - \langle r_j \rangle^2\right)}} \tag{2}$$

where C_{ij} represents the correlation between index i and j while <…> denotes the statistical average of its constituent. In this study, N comprises of 13 indexes. Therefore, a 13×13 dimensioned cross-correlation characterised by $\frac{13(13-1)}{2} = 78$ correlation coefficients completely, with values ranging from -1 to 1, is constructed and visualised through a correlogram. This correlogram visually highlights the most and least correlated indexes.

3.3 Setting the Threshold Value

The cross-correlation-based threshold network approach in this study involves computing a threshold value, θ, ranging from -1 to 1, based on the respective cross-correlation coefficients for each period. When the cross-correlation coefficient among two indexes exceeds θ, an edge materialises between them. In other words, when edges have weights below the threshold value or C_{ij} < θ, these edges are removed, rendering networks with the same number of nodes but a different number of edges depending on the threshold value set. To construct the threshold networks, we adopt two dynamic threshold values for each year: (i) the average correlation ($\bar{C}$) and (ii) $\bar{C}$ + one standard deviation (σ). These values are derived using Fisher's z-transformation to correct the downward bias in averaging correlation coefficients (Silver & Dunlap, 1987). The resulting z-scores are then back-transformed to obtain more accurate threshold levels that reflect the underlying correlation structure of each subperiod.

All networks constructed are undirected and unweighted, where an edge is present if the correlation between two sector indices exceeds the threshold. This approach permits a more nuanced representation of market interconnectedness than alternatives such as the Minimum Spanning Tree (MST) or Planar Maximally Filtered Graph (PMFG). While MST ensures full connectivity with the minimum number of edges, it may overlook meaningful but weaker connections. PMFG addresses this partially by including more edges but imposes planarity constraints. In contrast, the threshold network method enables tailored network sparsity and more realistic modelling of structural changes across both volatile and stable market periods.

Fisher's z transformation in Equation 3 can almost completely correct this skew, followed by the computation of these z values' mean. Even though the distribution of z may be approximately normal, it tends to overestimate the population value. Thus, using Equation 4, the inverse Fisher transform is applied to back transform the average of z into a correlation coefficient, which appears to be less biased than simply averaging correlation coefficients. This final value in the form of a correlation coefficient, denoted as $\bar{C}$, is the mean of the correlation matrix used. Thus, $\bar{C}$ and $\bar{C} + \sigma$ are set as the threshold values for each network. The Fisher's z transformation (Fisher, 1934) and inverse Fisher transform formulas are as follows:

$$z = 0.5\ln\left[\frac{(1+C)}{(1-C)}\right], \tag{3}$$

where C is the cross-correlation coefficient and z is the Fisher's z as follows

$$\bar{C} = \frac{(e^{2z}-1)}{(e^{2z}+1)}, \tag{4}$$

3.4 Centrality Measures

According to Luke (2015), in non-directed networks, centrality refers to nodes (indexes) that are in a central or influential position as they have many direct or indirect relationships with other nodes. Influential indexes in this study are determined based on degree, closeness, betweenness and eigenvector centrality measures. Since these measures are determined through different mathematical computations on the same underlying data, the top indexes across measures may or may not vary. By far, the degree centrality, $C_D(i)$, is the simplest measure of centrality in that it is merely the number of nodes a node is connected to. The degree centrality of index i is calculated as follows (Freeman, 1978):

$$C_D(i) = \frac{\sum_{j}^{N} A_{ij}}{N-1} \tag{5}$$

where $A_{ij} = 1$ if and only if index i and j have an edge between them and $A_{ij} = 0$ otherwise.

Next, the closeness centrality, $C_C(i)$, focuses on how close each node is to all the other nodes in a particular network. By definition, a node is more influential if they are close to every other node in said network. Mathematically, closeness centrality can be defined as

$$C_C(i) = \left[\sum_{j=1}^{N} d(i, j) \right]^{-1}, \tag{6}$$

with $d(i,j)$ being the number of edges in the geodesic connecting index i and j.

A node possesses high betweenness if other nodes need to pass through it to reach each other. This centrality is important as it enables the control of information flow in networks. For computation, the following formula is used:

$$C_B(i) = \sum_{h<k}^{N} \frac{b_{hk}(i)}{b_{hk}}, h \neq k \neq i \ , \tag{7}$$

with b_{hk} being the number of geodesics connecting index h and k, whereas $b_{hk}(i)$ is the same thing inclusive of passing through index i.

Lastly, there is the concept of eigenvector centrality, which considers a node influential if it is connected to other nodes that are themselves influential. Eigenvector centrality is expressed as shown below:

$$Eig(i) = \lambda^{-1} \sum_{j=1}^{N} A_{ij} x_j, i = 1, 2, ..., N. \tag{8}$$

Moreover, Equation 8 can also be written as:

$$A_{ij} Eig(i) = \lambda Eig(i) \ , \tag{9}$$

where A_{ij} is an adjacency matrix while *Eig(i)* is an eigenvector of the largest eigenvalue, λ.

4.0 Results and Discussion

Section 3 presents the threshold networks of the Bursa Malaysia sectoral indexes for the years 2019, 2020, and 2021. Before displaying the threshold networks, a descriptive analysis consisting of charts and correlograms are presented to enhance one's understanding of the pandemic's impact. A thorough discussion on centrality measures and topological properties of the network throughout the years can also be found in this section.

4.1 Descriptive Analysis

A descriptive statistical analysis was performed on thirteen sectoral indices listed on Bursa Malaysia from 2019 to 2021 to examine their performance, variability, and distributional characteristics. The analysis revealed notable heterogeneity across sectors in terms of central tendency and dispersion. The Financial Services (KLFI) and Healthcare (KLHC) indices recorded the highest average values, with KLFI showing a mean of 14,961.28 and KLHC reflecting elevated volatility with a standard deviation exceeding 1,000 points. Conversely, indices such as Technology (KLCT) and Telecommunications (KLTE) reported much lower mean values, consistent with their comparatively smaller market representation. The proximity between the mean and median in most indices indicates relatively symmetric distributions, although deviations in KLTE and KLHC suggest the presence of skewness.

Regarding distributional shape, several indices exhibited mild skewness—both positive and negative with the Utilities sector (KLUT) showing the most pronounced negative skew (–1.025), implying a higher frequency of extreme low values. The kurtosis values for all indices were below three, indicating platykurtic distributions with flatter shapes and lighter tails compared to a normal distribution. This suggests that extreme market movements were less frequent across most sectors. However, KLUT displayed a relatively high kurtosis (1.741), indicating a moderate peak concentration. Overall, the findings highlight diverse risk-return profiles across Bursa Malaysia's sectors, emphasising the need for sector-specific approaches in investment and risk management strategies.

In addition to descriptive statistics, we assess sector-specific volatility using standard deviation and maximum drawdown across the study period. The Financial Services index (KLFI) exhibited the highest volatility, with a standard deviation of

1,489.37 points and a maximum drawdown of approximately 39% in early 2020. Similarly, KLHC (Healthcare) saw a steep rise followed by a sharp correction, highlighting pandemic-driven speculative activity. In contrast, sectors such as KLIP (Industrial Products) and KLCT (Construction) maintained relatively stable price trends, with lower variance and minimal drawdowns. These observations are consistent with the defensive and cyclical nature of respective sectors and underscore heterogeneous market reactions during the pandemic.

Table 2: Descriptive Analysis

Indices	Mean	Sd	Median	Min	Max	Skew	Kurtosis
KLCT	180.998	21.346	175.170	121.910	227.460	0.285	-0.759
KLCM	615.533	46.748	613.790	466.270	709.130	-0.272	-0.458
KLEN	906.259	173.454	864.260	513.750	1291.250	0.387	-0.919
KLFI	14961.276	1489.373	15187.090	10885.450	17878.470	-0.335	-0.417
KLHC	2280.614	1025.161	2274.170	1142.400	4456.090	0.380	-1.335
KLIP	163.616	25.347	161.410	92.520	213.410	-0.168	-0.540
KLPL	6898.545	384.972	6939.630	5532.030	7849.640	-0.502	0.074
KLPR	745.460	103.567	736.530	495.190	964.600	0.233	-0.706
KLRE	891.033	79.433	856.910	778.050	1018.540	0.282	-1.623
KLTE	56.318	24.494	43.490	23.810	100.860	0.467	-1.403
KLTC	658.136	49.250	668.250	483.540	747.720	-0.705	-0.123
KLTP	763.297	82.185	766.840	480.710	936.010	-0.490	0.460
KLUT	948.836	43.436	955.140	752.780	1034.570	-1.025	1.741

The line chart in Figure 1 illustrates trends in closing prices of all 13 sectorial indexes from January 1 2019 to December 31 2021. Overall, all 13 indexes have a kink in their curve around the time the MCO was implemented, indicating how the pandemic had an immediate effect in causing the stock market to record its lowest point in years. Aside from KLHC, KLIP and KLTE, the other indexes seem to record stable closing prices after the sudden drop. On the other hand, KLHC's closing prices rise to a peak in the third quarter of 2020 before slowly falling. Not the same can be said for KLIP and KLTE, in which closing prices show an upward trend after the drop, even though they are among the two sectorial indexes with the smallest closing prices in general. In 2021, KLIP even managed to overtake the closing prices of KLCT, which had higher closing prices all the while.

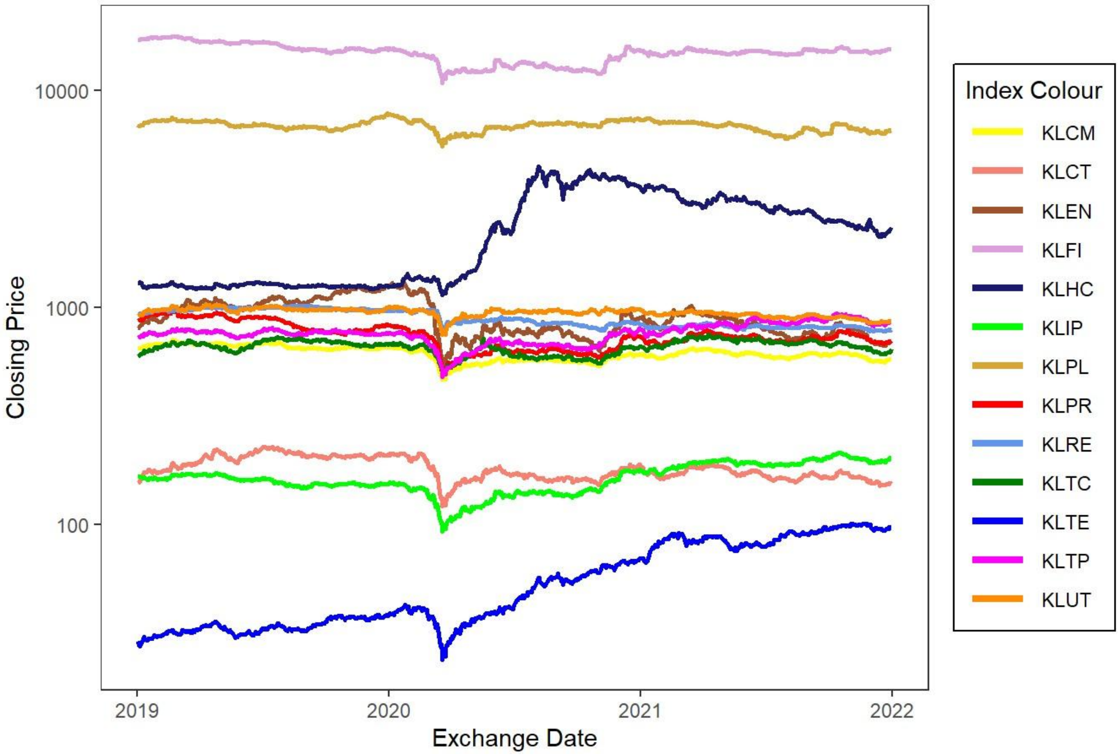

Figure 1: Sectoral Index Closing Prices (2019–2021)

Next, Figure 2 illustrates the average rate of return for all 13 indexes over three years in the form of a faceted bar chart. Only four indexes, namely KLFI, KLHC, KLIP, and KLTE, recorded increases in the average rate of return in 2020, whereas the other indexes were negatively affected. However, these increases do not maintain their trend throughout 2021. From this figure, it is very clear that KLHC thrived in the year 2020 compared to the other indexes, recording an average rate of return of a little over 0.4%. This promising rate of return however, was short-lived as KLHC's average rate of return in the following year plummeted to almost -0.2%, making it the worst drop out of all the indexes. Coming in second, KLTE showed a 0.13% increase in the average rate of return from 2019 to 2020 before dropping 0.11% in 2021, not nearly as much as KLHC's drop.

Also noteworthy, KLEN took the biggest downfall in 2020 when it recorded a drop of 0.31% in its average rate of return. This faceted bar chart provides a little insight into the dramatic changes taking place in the average rates of return of the stock market when facing crisis.

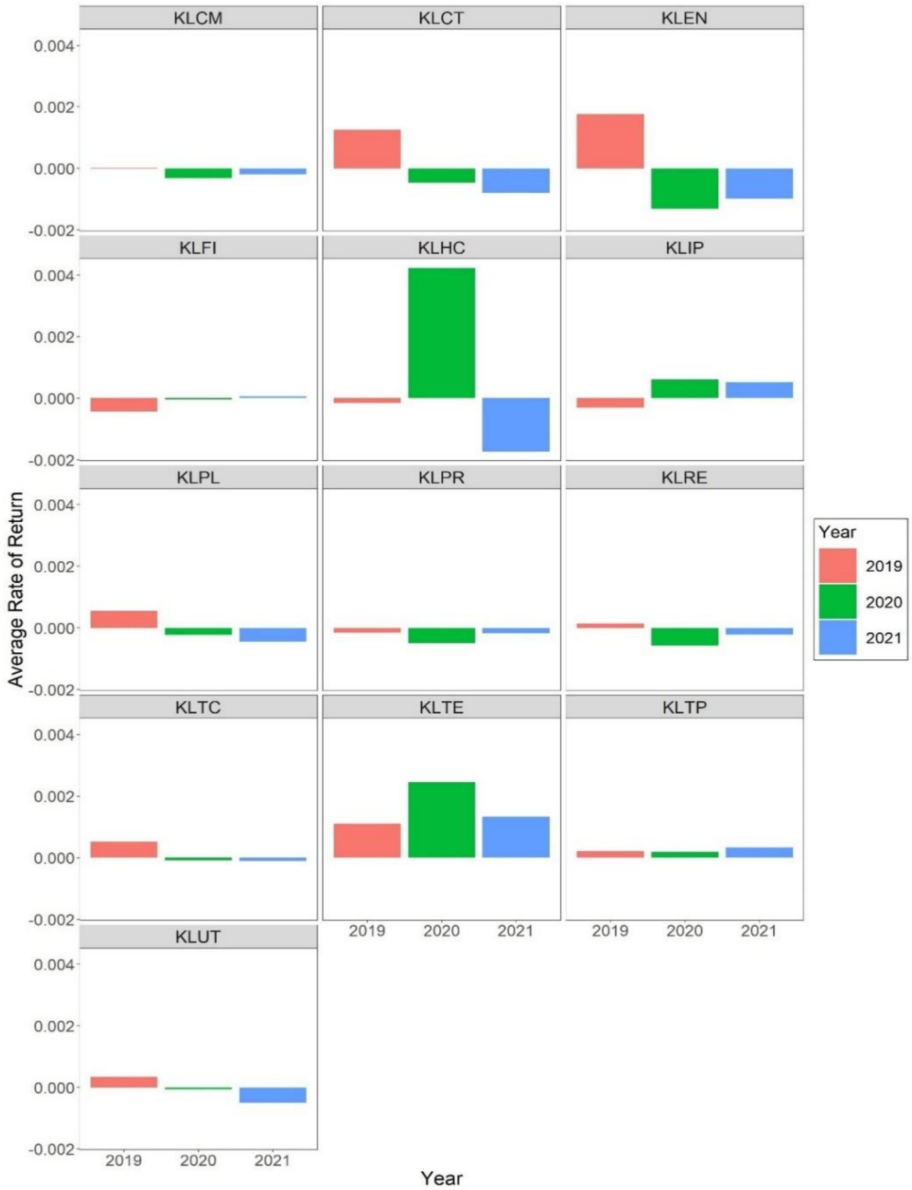

Figure 2: Average Annual Rates of Return by Sector (2019–2021)

To inspect and visualise the correlation matrices of the 2019, 2020 and 2021 networks, correlograms are plotted in Figure 3, Figure 4 and Figure 5, respectively. Correlation coefficients can range from -1 to 1, with -1 being a perfect negative correlation and 1 being a perfect positive correlation. In the three correlograms below, the blue colour represents positive correlations. In contrast, the red colour represents negative correlations, and the x and y axes display all 13 indexes of the Malaysian stock market. Note that the correlogram is symmetric along the diagonals, all of which amount to correlation values of 1, since they represent the correlation of an index with itself. An initial observation of these figures displays discernible changes in the correlation structure over the years. Figure 3 reveals the correlation among indexes in the year 2019. From a glance, most of the indexes have correlations between 0.25 to 0.5. It can be seen that only one pair of nodes are negatively correlated, namely KLFI and KLRE, with a value of 0.057. KLCT and KLPR, on the other hand, have the most significant correlation of 0.561.

Moving on to Figure 4, the correlogram depicts more pairs of indexes having stronger correlations between 0.5 and 0.75 in the year 2020. Taking a huge leap in value, KLCM and KLIP have the strongest relationship with a value of 0.804. Even the weakest link in 2020, between KLFI and KLHC, has a positive correlation of 0.106, which indicates that no indexes were negatively correlated. In 2021, the relationships between indexes start to weaken once again. The weakest link in 2020 experienced a change in correlation direction, besides two other pairs becoming negatively correlated, namely KLEN and KLHC, besides KLHC and KLRE. All the negatively correlated relationships are associated with KLHC. As seen throughout the years during the pandemic, the direction of correlations did not change drastically, but not the same can be said about the strength of the relationships. The years 2019 and 2021 showed lower average correlation values, therefore emphasising relatively weaker clusters compared to the year 2020.

During the year 2020, besides not having any negative correlations, the indexes are more interconnected with each other, as can also be seen in the network plots of the next subsection. Similar to a study by Memon (2022), during volatile periods of time like the COVID-19 outbreak, indexes tend to cluster as there is a tight correlation among indexes, and thus, they move in a homogenous direction. Having said that, correlograms can assist investors in analysing the relationship between indexes before making an investment decision. The closing prices of KLCT had consistently higher closing prices.

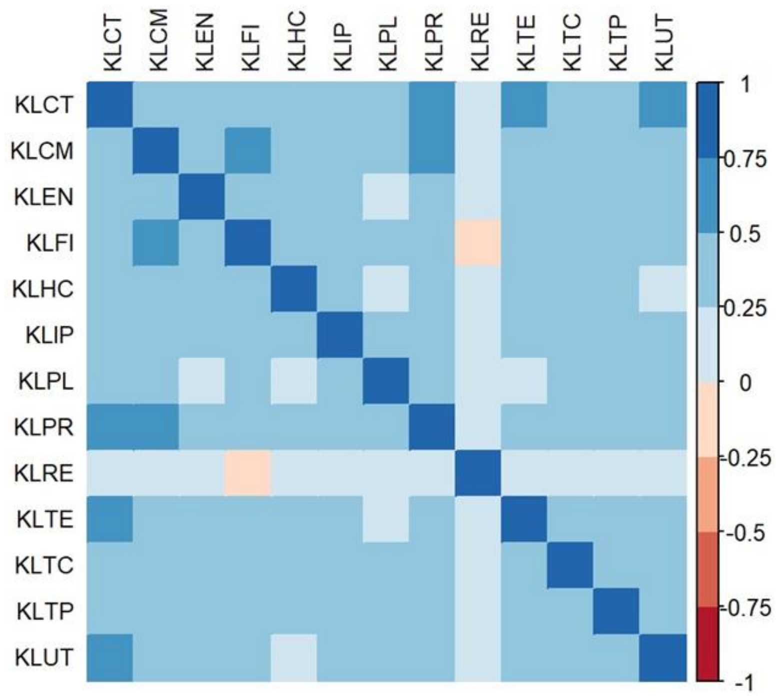

Figure 3: 2019 Sectoral Correlation Matrix (Correlation Range: –0.05 to 0.56)

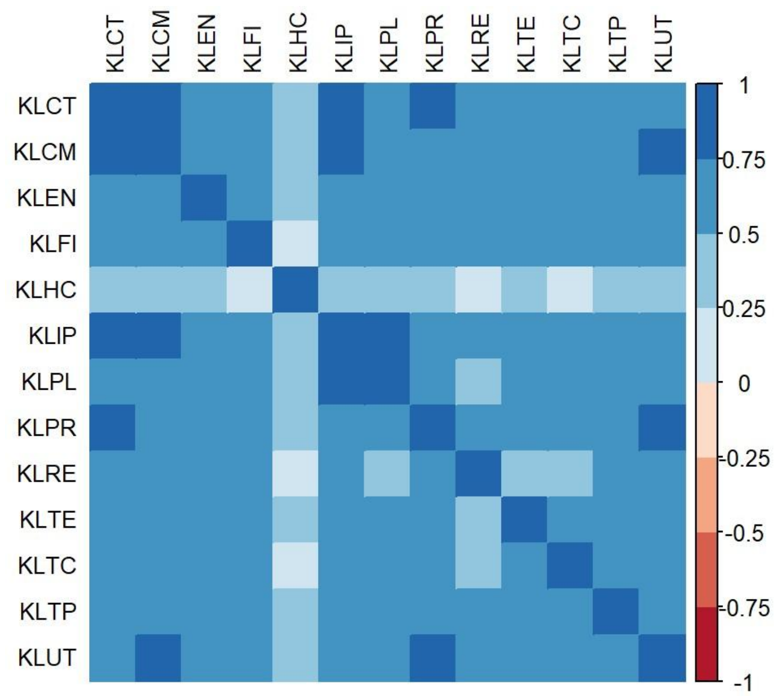

Figure 4: 2020 Sectoral Correlation Matrix (Correlation Range: 0.10 to 0.80)

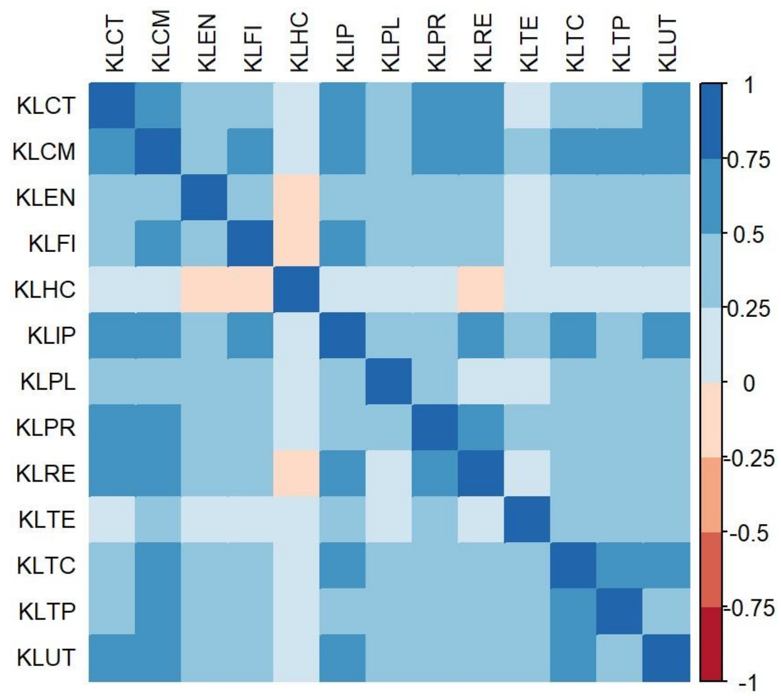

Figure 5: 2021 Sectoral Correlation Matrix (Correlation Range: –0.15 to 0.70)

4.2 Threshold Networks

In this subsection, evolution of the threshold networks for the years 2019, 2020 and 2021 at different threshold values can be viewed. The nodes are denoted as indexes, while the edges that connect nodes represent correlations between indexes. Figure 6, Figure 7 and Figure 8 portray threshold networks constructed at a threshold value of the mean of the correlation matrix, $\bar{C}$, whereas Figure 9, Figure 10, and Figure 11 portray threshold networks constructed at a threshold value of mean plus one standard deviation of the correlation matrix, $\bar{C}+\sigma$, for each subperiod respectively.

Figure 6 portrays the 2019 threshold network constructed at a threshold value of 0.161. It can be seen that the KLRE index is disconnected from the other nodes, which are interconnected to each other. Each of the 12 interconnected indexes were connected to each other as all of them had 11 edges each. In the following year, Figure 7 portrays a threshold network with a threshold value that doubled to 0.321. The disconnected node from 2019, KLRE, has joined the other nodes, forming a single main group and altering the network's structure. KLCT, KLIP, KLPR, KLTE, KLTP, and KLUT remained as the key nodes, each sharing the same number of edges, which is 12. This indicates that all the indexes are connected to these six indexes in 2020. Notably, KLHC, with only 6 edges, was the least influential node. For the year 2021, Figure 8 represents the threshold network that was constructed at a threshold value of 0.179. Following a decreasing trend in its number of connections, KLHC lost all its connections in 2021, leading to its disconnection from the rest of the nodes. Furthermore, KLCT, KLIP, KLPR, KLTP, KLUT continue to remain key nodes, with KLCM, KLFI, KLRE and KLTC being added to the list, each consisting of 11 edges.

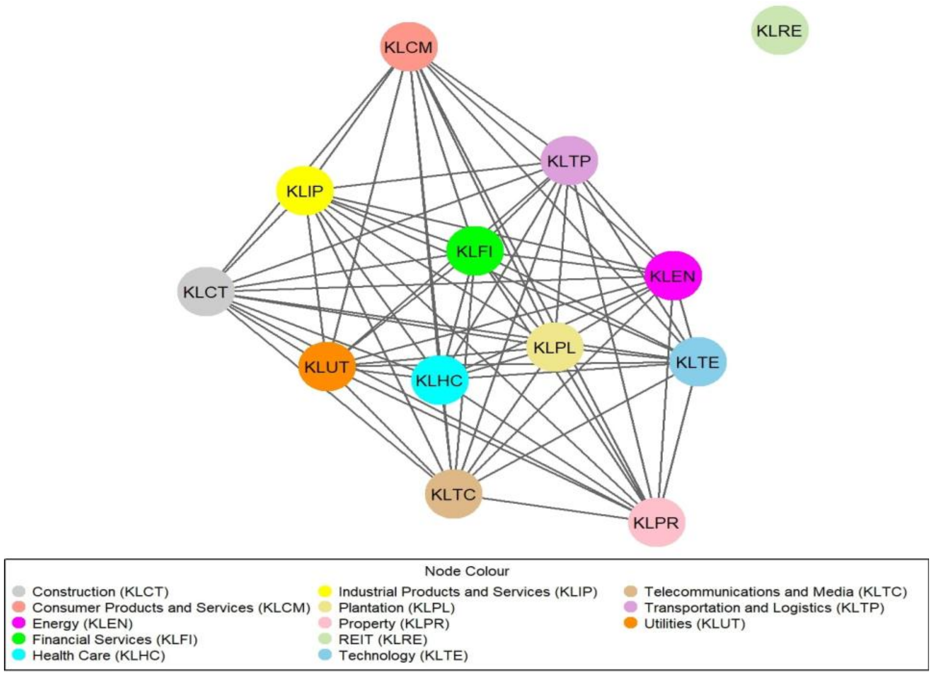

Figure 6: 2019 Threshold Network ($\overline{C}$= 0.161)

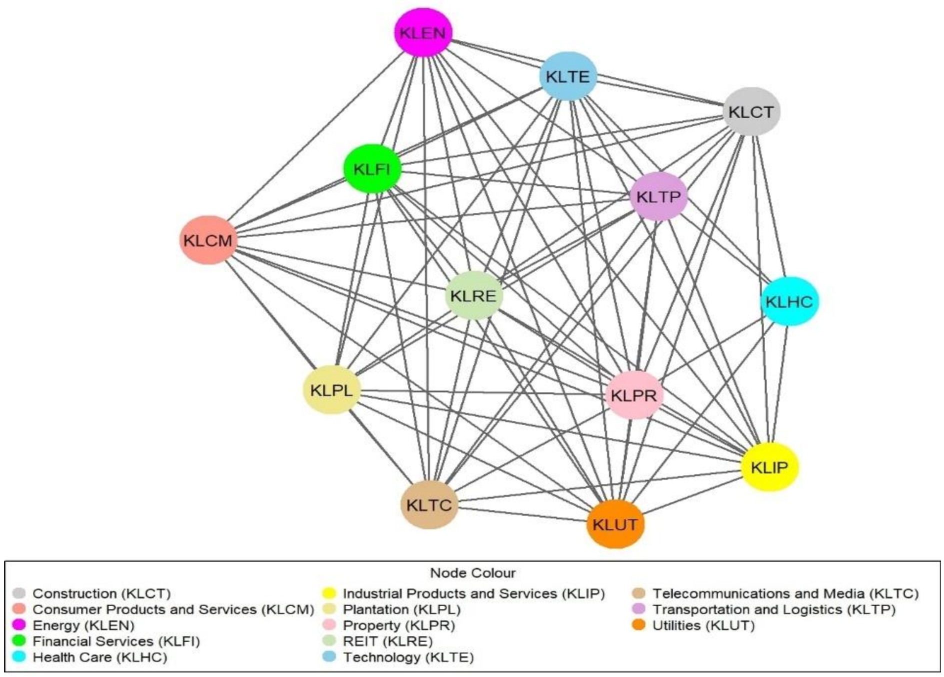

Figure 7: 2020 Threshold Network ($\overline{C}$ = 0.321)

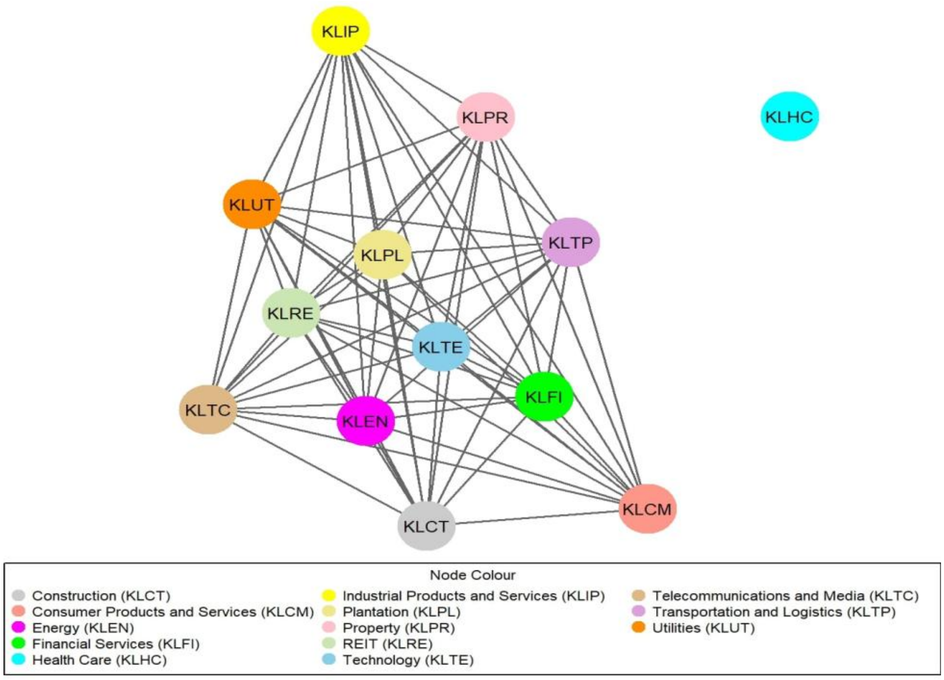

Figure 8: 2021 Threshold Network ($\overline{C}$ = 0.179)

Moving the threshold value up a notch, the threshold networks are constructed at a higher value of mean plus one standard deviation of the correlation matrix. Figure 9 displays a threshold network constructed at 0.350, Figure 10 displays a threshold network constructed at 0.638, and Figure 11 displays a threshold network constructed at 0.396 for the years 2019, 2020 and 2021, respectively. Similar to the 2019 threshold network, even with a higher cut-off point, KLRE remains the sole index disconnected from the main group, which is now less interconnected. The most influential index is KLCM, with 10 edges, followed by KLIP, KLCT, and KLPR, each with 9 edges. For the 2020 and 2021 threshold networks, on the other hand, KLHC has no edges whatsoever, disconnecting it from the other nodes. As seen in 2019, KLCM remains the key node with 11 edges, followed by KLIP and KLPR, which each have 10 edges for the year 2020. However, in 2021, there is a slight change, with KLIP and KLCM switching places as the most connected indexes. In this network, KLIP has 11 edges, whereas KLCM has 10.

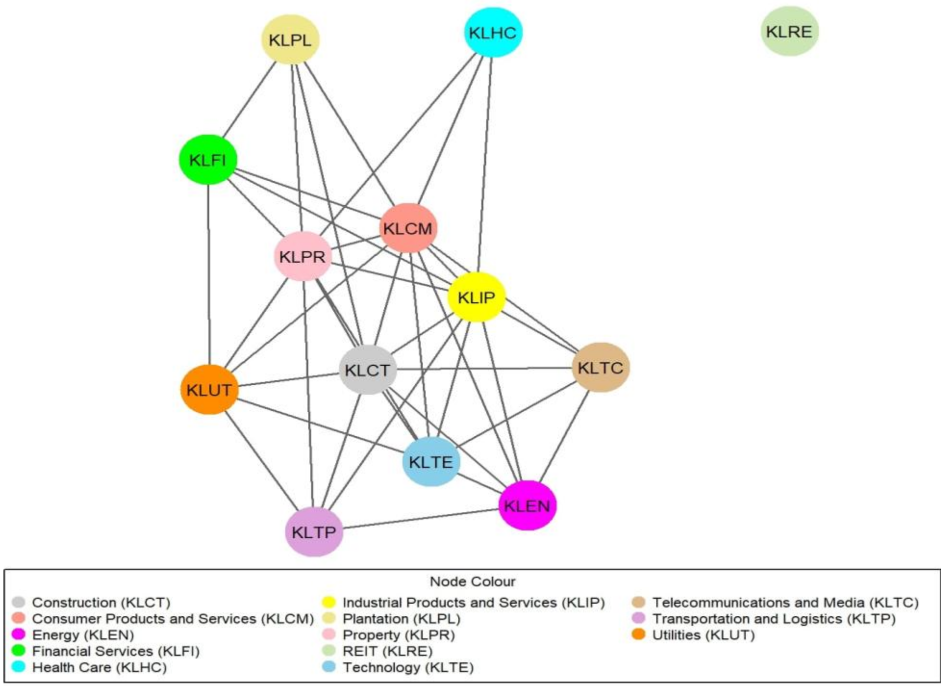

Figure 9: 2019 Threshold Network ($\bar{C} + \sigma = 0.350$)

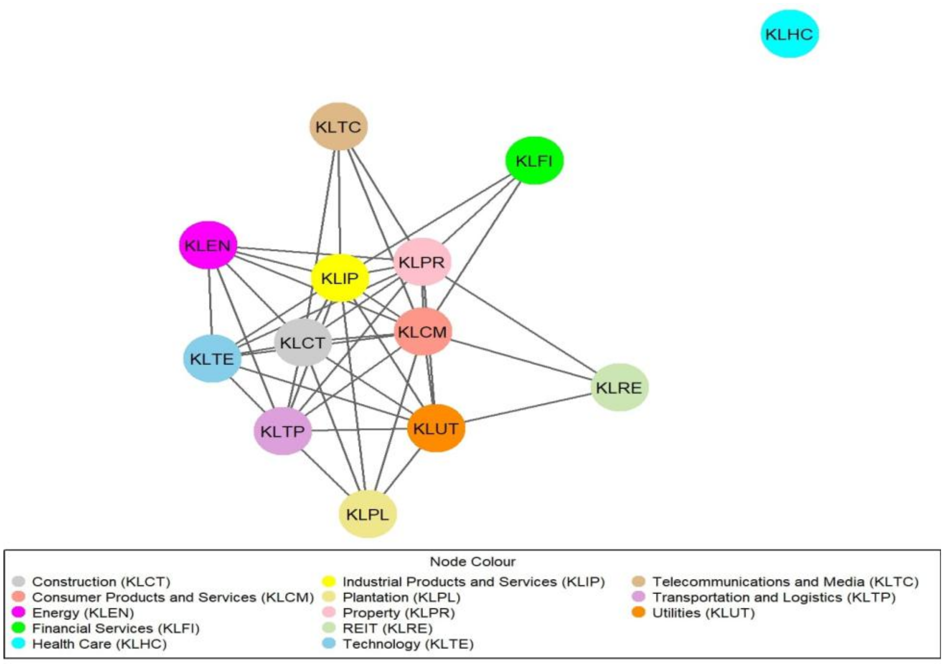

Figure 10: 2020 Threshold Network ($\bar{C} + \sigma = 0.638$)

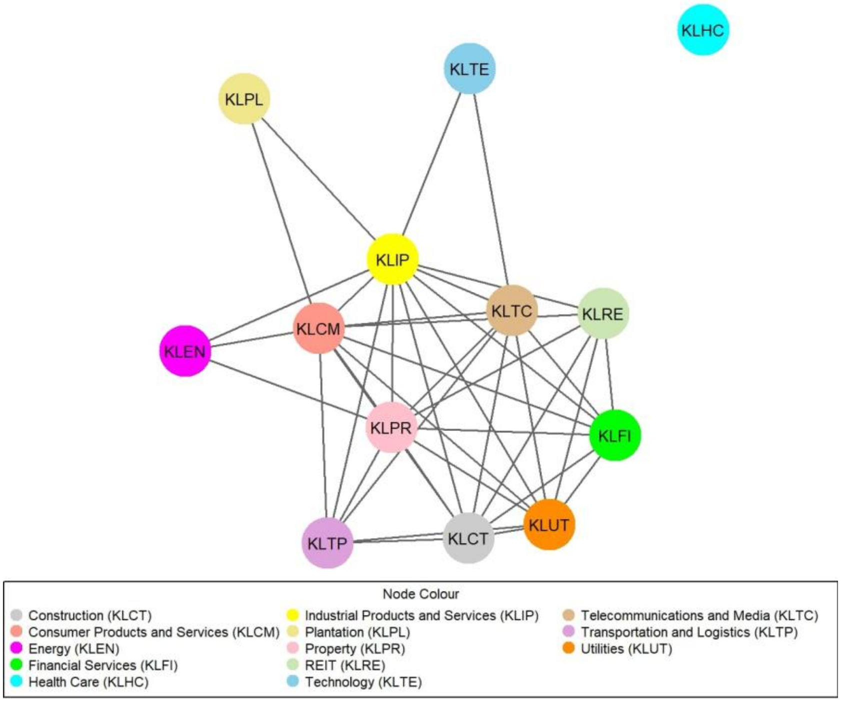

Figure 11: 2021 Threshold Network ($\overline{C} + \sigma = 0.396$)

Comparing threshold networks constructed from a threshold value of C¯ and C¯+σ, it can be said that as the threshold value increases, the networks appear to be less dense. This provides a clearer picture of the connections between each index, facilitating better interpretations and informed decisions. For each threshold network, the results seem to be fairly consistent, with the KLRE index being disconnected in 2019 and the KLHC index being disconnected for the other years. There is, however, an exception for the 2020 threshold network constructed from the mean of the correlation matrix, as the threshold value was too low to enable KLHC to be cut off. Nevertheless, KLHC still had the least number of connections, so it was on its way to being disconnected with a little increase in threshold value anyway. Throughout the years, KLCM, KLIP, KLPR, and KLCT tend to stand out as the indexes with the most connections, given that they are the four indexes with the greatest number of constituents. In short, the positions of the indexes remain intact even as threshold values increase, as no extra indexes were cut off.

4.3 Degree Centrality

The first measure of centrality used to identify the most influential stocks of the threshold networks is the degree centrality. The higher the number of edges a node has, the more influential that particular node is in terms of degree centrality. Table 2 and Table 3 reveal the indexes in decreasing order of degree values for all three years based on a threshold value of $\bar{C}$ and $\bar{C}+\sigma$ respectively. It appears from Table 2 that KLCT, KLIP, KLPR, KLTP and KLUT remain as nodes with the highest degree values throughout all three years. These five indexes had degree values of 11 in 2019, which then increased by one in 2020 before falling back to 11 in 2021. Table 3 further depicts the top indexes of threshold networks constructed from $\bar{C}+\sigma$. This table reveals that four indexes consistently appear in the top four spots for the highest degree values: KLCM, KLIP, KLPR, and KLCT. They always appear in this order except in 2021, where KLIP ranks first, and KLCM falls to the second spot. KLCM starts off with 10 edges in 2019 to 11 edges in 2020 before dropping back to 10 the following year. For its tight competitor, KLIP starts off with 9 edges in 2019 and increases by one edge each in 2020 and 2021. It can be concluded that for both threshold values, KLCM, KLIP, KLPR and KLCT remain selected as indexes in the top four, indicating that they are the least impacted by the pandemic.

Table 3: Degree Centrality Values for Threshold Networks Constructed using a Threshold Value of $\bar{C}$

No	Degree 2019		Degree 2020		Degree 2021	
1	KLCT	11.000	KLCT	12.000	KLCT	11.000
2	KLCM	11.000	KLIP	12.000	KLCM	11.000
3	KLEN	11.000	KLPR	12.000	KLFI	11.000
4	KLFI	11.000	KLTE	12.000	KLIP	11.000
5	KLHC	11.000	KLTP	12.000	KLPR	11.000
6	KLIP	11.000	KLUT	12.000	KLRE	11.000
7	KLPL	11.000	KLCM	11.000	KLTC	11.000
8	KLPR	11.000	KLEN	11.000	KLTP	11.000
9	KLTE	11.000	KLFI	11.000	KLUT	11.000
10	KLTC	11.000	KLPL	11.000	KLEN	10.000
11	KLTP	11.000	KLRE	11.000	KLPL	10.000

12	KLUT	11.000	KLTC	11.000	KLTE	9.000
13	KLRE	0.000	KLHC	6.000	KLHC	0.000

Table 4: Degree Centrality Values for Threshold Networks Constructed using a Threshold Value of $\bar{C} + \sigma$

No	Degree 2019		Degree 2020		Degree 2021	
1	KLCM	10.000	KLCM	11.000	KLIP	11.000
2	KLCT	9.000	KLIP	10.000	KLCM	10.000
3	KLIP	9.000	KLPR	10.000	KLPR	9.000
4	KLPR	9.000	KLCT	9.000	KLCT	8.000
5	KLTE	7.000	KLTP	8.000	KLTC	8.000
6	KLEN	6.000	KLUT	8.000	KLUT	8.000
7	KLUT	6.000	KLTE	7.000	KLFI	7.000
8	KLFI	5.000	KLEN	6.000	KLRE	6.000
9	KLTC	5.000	KLPL	5.000	KLTP	6.000
10	KLTP	5.000	KLTC	4.000	KLEN	3.000
11	KLPL	4.000	KLFI	3.000	KLPL	2.000
12	KLHC	3.000	KLRE	3.000	KLTE	2.000
13	KLRE	0.000	KLHC	0.000	KLHC	0.000

4.4 Closeness Centrality

Normally, closeness centrality is higher for nodes that are closer to all the other nodes in a network. Based on the definition, nodes with high closeness values can quickly disseminate information to other nodes. From the analysis carried out, the closeness centrality of all six threshold networks arranged in decreasing order can be found in Table 4 and Table 5. Starting off with threshold networks constructed from a threshold value of $\bar{C}$, the analysis reveals that KLPL and KLHC tie with the most significant closeness value amounting to 0.061. In the next year, the first-place ranking was remarkably replaced by KLRE, which came from the last spot in 2019. KLPL dropped to the fifth position, whereas KLHC plummeted even further to the tenth position, even though both showed an increase in value. In the final subperiod, however, KLPL reclaimed its top spot with a similar value of 0.060, being tailed by KLTE with a value of 0.059 in second place. On the other hand, KLHC continued its downward trend, taking up the last spot in 2021 with a small closeness value of 0.006.

Moving forward, Table 5 illustrates how KLIP became the top scorer in 2019, with a closeness value of 0.055, before losing its position to KLCM in 2020, with a value of 0.048. In 2021, KLIP regained the top spot, jumping from third place with a closeness value of 0.060. Summing up, the findings from Table 4 show that there are no consistent indexes listed in the top five throughout the three years for the $\bar{C}$ threshold networks except for KLPL. To the contrary, KLIP, KLPR, KLCM and KLCT consistently appear in the top five spots of the 2019, 2020 and 2021 networks with a threshold value of $\bar{C}+\sigma$. This illustrates how all the indexes were closely linked to these four indexes within their respective networks.

Table 5: Closeness Centrality Values for Threshold Networks Constructed using a Threshold Value of $\bar{C}$

No	Closeness 2019		Closeness 2020		Closeness 2021	
1	KLHC	0.061	KLRE	0.138	KLPL	0.060
2	KLPL	0.061	KLTE	0.134	KLTE	0.059
3	KLFI	0.059	KLTP	0.134	KLEN	0.058
4	KLTC	0.059	KLTC	0.132	KLFI	0.057
5	KLTP	0.059	KLPL	0.130	KLRE	0.057
6	KLUT	0.059	KLCT	0.129	KLTP	0.057
7	KLEN	0.058	KLFI	0.129	KLCT	0.056
8	KLIP	0.058	KLPR	0.129	KLPR	0.056
9	KLTE	0.058	KLUT	0.128	KLTC	0.056
10	KLPR	0.057	KLHC	0.127	KLUT	0.056
11	KLCT	0.056	KLEN	0.126	KLIP	0.054
12	KLCM	0.056	KLIP	0.126	KLCM	0.053
13	KLRE	0.006	KLCM	0.111	KLHC	0.006

Table 6: Closeness Centrality Values for Threshold Networks Constructed using a Threshold Value of $\bar{C} + \sigma$

No	Closeness 2019		Closeness 2020		Closeness 2021	
1	KLIP	0.055	KLCM	0.048	KLIP	0.054
2	KLCT	0.054	KLPR	0.047	KLPR	0.052
3	KLCM	0.054	KLIP	0.046	KLCM	0.051
4	KLPR	0.053	KLCT	0.045	KLTC	0.051
5	KLTE	0.052	KLTP	0.045	KLCT	0.050
6	KLEN	0.051	KLUT	0.044	KLFI	0.050
7	KLFI	0.051	KLTE	0.043	KLUT	0.050
8	KLUT	0.051	KLEN	0.042	KLTP	0.049
9	KLPL	0.050	KLPL	0.041	KLRE	0.048
10	KLTC	0.050	KLTC	0.040	KLEN	0.046
11	KLTP	0.050	KLFI	0.039	KLPL	0.045
12	KLHC	0.049	KLRE	0.039	KLTE	0.045
13	KLRE	0.006	KLHC	0.006	KLHC	0.006

4.5 Betweenness Centrality

The third centrality measure is betweenness centrality, which is displayed in decreasing order for all three subperiods with different threshold values in Tables 6 and 7. As the betweenness value of a node increases, the ability of the node to dominate information flow within a network increases. Beginning from Table 6, only KLPL has a non-zero betweenness value of 1 in 2019. KLPL then displays a value of 0 in 2020 before being in the top four indexes once again in 2021. For the year 2020, KLHC takes the lead with a betweenness value of 9, followed closely by KLTP, which lags behind by 5 points. The consecutive year then proceeds to be topped by KLTE with a value of 4.

Across threshold networks constructed using a threshold value of $\bar{C} + \sigma$, KLIP was the highest ranked in 2019 and 2020, with betweenness values of 8 and 13, respectively. Anyway, KLIP dropped to the sixth position (tying with the fifth position) in 2020, leaving the first place to be claimed by KLPR with a value of 11. From Table 7, KLIP, KLCT and KLPR remain named as the top five scorers, indicating how they have high intermediary influence over the network. This does not apply to threshold networks constructed using a threshold value of $\bar{C}$ as their top scorers change with no particular pattern.

Table 7: Betweenness Centrality Values for Threshold Networks Constructed using a Threshold Value of $\overline{C}$

No	Betweenness 2019		Betweenness 2020		Betweenness 2021	
1	KLPL	1.000	KLHC	9.000	KLTE	4.000
2	KLCT	0.000	KLTP	4.000	KLFI	1.000
3	KLCM	0.000	KLIP	1.000	KLPL	1.000
4	KLEN	0.000	KLPR	1.000	KLRE	1.000
5	KLFI	0.000	KLCT	0.000	KLCT	0.000
6	KLHC	0.000	KLCM	0.000	KLCM	0.000
7	KLIP	0.000	KLEN	0.000	KLEN	0.000
8	KLPR	0.000	KLFI	0.000	KLHC	0.000
9	KLRE	0.000	KLPL	0.000	KLIP	0.000
10	KLTE	0.000	KLRE	0.000	KLPR	0.000
11	KLTC	0.000	KLTE	0.000	KLTC	0.000
12	KLTP	0.000	KLTC	0.000	KLTP	0.000
13	KLUT	0.000	KLUT	0.000	KLUT	0.000

Table 8: Betweenness Centrality Values for Threshold Networks Constructed using a Threshold Value of $\overline{C}+\sigma$

No	Betweenness 2019		Betweenness 2020		Betweenness 2021	
1	KLIP	8.000	KLPR	11.000	KLIP	13.000
2	KLCT	4.000	KLTP	4.000	KLPR	5.000
3	KLPR	3.000	KLUT	4.000	KLTC	4.000
4	KLTE	3.000	KLCM	3.000	KLCT	2.000
5	KLUT	3.000	KLCT	1.000	KLCM	1.000
6	KLCM	2.000	KLIP	1.000	KLFI	1.000
7	KLFI	2.000	KLEN	0.000	KLEN	0.000
8	KLEN	1.000	KLFI	0.000	KLHC	0.000
9	KLTP	1.000	KLHC	0.000	KLPL	0.000
10	KLHC	0.000	KLPL	0.000	KLRE	0.000
11	KLPL	0.000	KLRE	0.000	KLTE	0.000
12	KLRE	0.000	KLTE	0.000	KLTP	0.000
13	KLTC	0.000	KLTC	0.000	KLUT	0.000

4.6 Eigenvector Centrality

The last centrality measure to be analysed is eigenvector centrality. Based on the concept of eigenvector centrality, a node is, in fact, influential if it is connected to other influential nodes. The eigenvector centrality measures sorted in decreasing order are depicted in Table 8 and Table 9 for all six threshold networks. Table 8 shows that KLCM has the highest score in 2019 and 2020. Unfortunately, dropping from a value of 1 to 0.996 in 2020 caused KLCM to fall into second place, relinquishing its spot to KLIP.

Table 11 presents a more promising picture, as KLCM continues to remain at the top with a value of 1 for all three years. KLCT took second place in 2019, falling short of 0.044 points behind KLCM. In 2020 and 2021, the largest sectoral index, known as KLIP, follows behind KLCM with values of 0.968 and 0.964, respectively. Interestingly, KLCM, KLIP, KLPR and KLCT were consistently topping the tables in all six threshold networks. Unquestionably, this is similar to the results of the degree centrality subsection, where these four indexes appear to be the most influential according to the concept of eigenvector centrality. To put it another way, KLCM, KLIP, KLPR, and KLCT are connected to many other influential indexes.

Table 9: Eigenvector Centrality Values for Threshold Networks Constructed using a Threshold Value of $\bar{C}$

No	Eigenvector 2019		Eigenvector 2020		Eigenvector 2021	
1	KLCM	1.000	KLIP	1.000	KLCM	1.000
2	KLCT	0.970	KLCM	0.996	KLIP	0.956
3	KLPR	0.957	KLCT	0.978	KLCT	0.869
4	KLIP	0.889	KLPR	0.976	KLPR	0.868
5	KLTE	0.889	KLUT	0.964	KLTC	0.855
6	KLEN	0.859	KLTP	0.929	KLUT	0.852
7	KLTP	0.848	KLTE	0.909	KLFI	0.807
8	KLTC	0.843	KLEN	0.886	KLTP	0.802
9	KLUT	0.828	KLFI	0.866	KLRE	0.793
10	KLFI	0.814	KLPL	0.863	KLEN	0.669
11	KLPL	0.738	KLTC	0.844	KLPL	0.598
12	KLHC	0.713	KLRE	0.811	KLTE	0.535
13	KLRE	0.000	KLHC	0.283	KLHC	0.000

Table 10: Eigenvector Centrality Values for Threshold Networks Constructed using a Threshold Value of $\overline{C} + \sigma$

No	Eigenvector 2019		Eigenvector 2020		Eigenvector 2021	
1	KLCM	1.000	KLCM	1.000	KLCM	1.000
2	KLCT	0.956	KLIP	0.968	KLIP	0.964
3	KLPR	0.903	KLPR	0.920	KLPR	0.862
4	KLIP	0.848	KLCT	0.911	KLCT	0.843
5	KLTE	0.817	KLUT	0.820	KLUT	0.830
6	KLEN	0.672	KLTP	0.819	KLTC	0.776
7	KLUT	0.661	KLTE	0.762	KLFI	0.733
8	KLTC	0.603	KLEN	0.657	KLRE	0.666
9	KLTP	0.559	KLPL	0.560	KLTP	0.644
10	KLFI	0.524	KLTC	0.446	KLEN	0.322
11	KLPL	0.431	KLFI	0.364	KLPL	0.230
12	KLHC	0.328	KLRE	0.338	KLTE	0.192
13	KLRE	0.000	KLHC	0.000	KLHC	0.000

4.7 Cross-Metric Summary of Top 4 Centrality Rankings (2019–2021) Based on a Threshold Value of $\overline{C} + \sigma$

To facilitate clearer interpretation, we focused on the performance of the top four sectoral indices based on centrality rankings (degree, closeness, betweenness, and eigenvector) from 2019 to 2021. These rankings were derived from networks constructed using the threshold value of $\overline{C} + \sigma$, which effectively captured year-to-year variations in sectoral influence. By limiting the analysis to the top-ranked sectors, the results highlight the most prominent market players while avoiding excessive technical detail. A cross-metric comparison, as in Table 11 and Figure 12 reveals that KLIP, KLPR, KLCM, and KLCT are consistently ranked among the top four most central indices across all three years (2019–2021). These sectors exhibit strong interconnectivity, high influence, and structural importance within Bursa Malaysia’s sectoral network during the pandemic. Their dominance is evident in degree, closeness, betweenness, and eigenvector centralities, reflecting robust and stable roles in sectoral dynamics. In contrast, KLHC and KLRE consistently occupy peripheral positions, highlighting their limited systemic influence during the observed period.

Table 11: Cross-Metric Summary of Top 4 Centrality Rankings

Sector	Degree	Closeness	Betweenness	Eigenvector	Total Top 4 Appearances
KLIP	3	3	3	3	12
KLPR	3	3	3	3	12
KLCM	3	3	1	3	10
KLCT	3	3	1	1	8

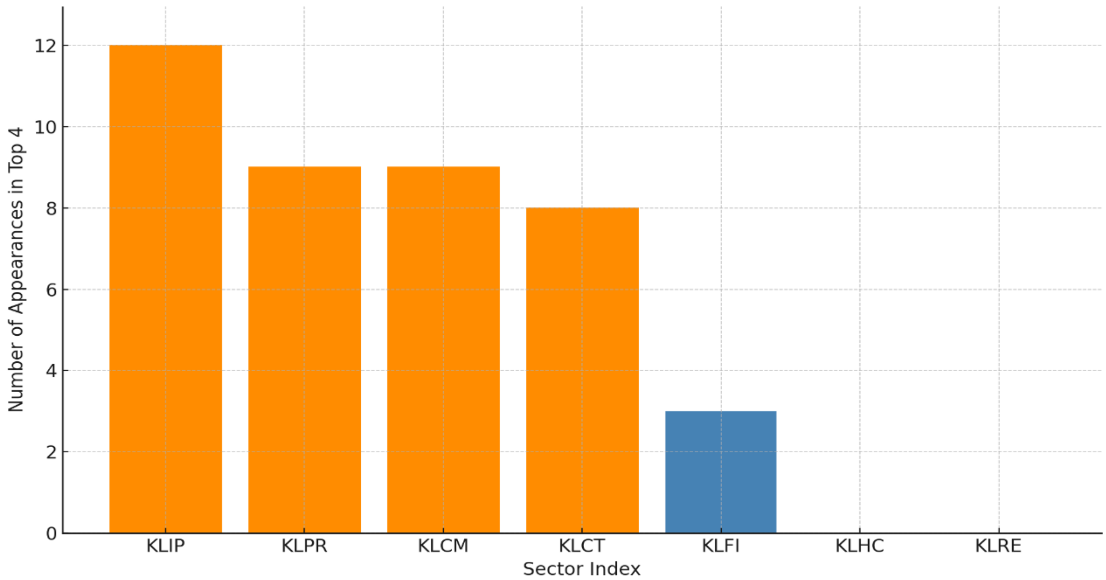

Figure 12: Frequency of Top 4 Rankings Across Centrality Measure based on a Threshold Value of $\overline{C} + \sigma$

4.8 Topological Properties

In summary, the topological properties of all six threshold networks are listed as displayed in Table 10. At a glance, this table indicates that with an increase in threshold values, the number of nodes in a network remains the same, regardless of the change. However, the number of edges in each network can vary, even if it is not that significant of a change. It can be seen that threshold networks in 2020 are more interconnected as they have the highest number of edges among all three years. With a higher threshold value, though, the networks tend to be sparser as more edges are cut off. Increasing the threshold value even more can provide additional insight into which indexes appear to be on the periphery of the networks.

Ranging from 0 to 1, the density of a network is the ratio of observed edges to the total number of potential edges (Luke, 2015). The density values recorded in Table 10 correspond to the number of edges where networks with more edges portray a higher density value. As the threshold value increases, the density of the network decreases significantly, as a higher threshold value corresponds to fewer edges. Subsequently, the diameter of a network refers to the longest geodesic distance spanning all node pairs. The highest diameter obtained from Table 10 is only 1.444 and 1.057, both from the 2020 networks. This indicates that all six threshold networks are quite compact, as it takes at most 1.444 steps to connect the two nodes that are placed the furthest from each other in the network with the highest diameter. Lastly, the ratio of closed triangles to the total number of open and closed triangles is known as transitivity. Seeing that threshold networks with a threshold value of $\bar{C}$ have higher transitivity values than threshold networks with a threshold value of $\bar{C} + \sigma$, it can be said that these networks have groups of nodes that are more densely connected internally, agreeing with the density values from earlier. In a nutshell, all the topological properties listed indicate that threshold networks constructed from the mean of the correlation matrix are more interconnected and compact compared to those constructed from the mean plus one standard deviation of the correlation matrix.

To provide a clearer comparative view of the network structure across different periods and thresholds, a heatmap of topological properties was constructed (Figure 13). The results reveal that network density and transitivity were highest in 2020 under the $\theta \geq \bar{C}$ condition, reflecting strong sectoral interconnectedness during the height of the COVID-19 pandemic. This suggests increased market homogeneity and heightened co-movement among sectors, potentially driven by systemic shocks and policy responses. Under the stricter threshold ($\theta \geq \bar{C} + \sigma$), the network became notably sparser across all years, with lower density and transitivity values, especially in 2019 and 2021. The network diameter peaked in 2020 under this threshold, indicating increased separation between the most distant sectors and a temporary breakdown in compactness. These topological shifts have important implications for financial contagion and diversification. High transitivity suggests that sectors tend to form tightly knit clusters, which can accelerate the transmission of shocks across interconnected nodes, thereby amplifying systemic risk. Similarly, a more compact network (with a lower diameter) facilitates faster information and volatility spillovers, thereby heightening contagion potential during crises. In contrast, the reduced transitivity and increased diameter observed under higher threshold conditions point to fragmentation and structural decoupling, which may enhance diversification opportunities by limiting synchronised sectoral responses. Understanding these dynamics is crucial for investors and regulators seeking to strike a balance between systemic stability and portfolio diversification during turbulent periods.

Table 10: Topological Properties of Six Threshold Networks of Bursa Malaysia Sectorial Indexes

Correlation	$\boldsymbol{\theta \geq \bar{C}}$			$\boldsymbol{\theta \geq \bar{C} + \sigma}$		
Period	**2019**	**2020**	**2021**	**2019**	**2020**	**2021**
Threshold Value	0.161	0.321	0.179	0.350	0.638	0.396
Number of Nodes	13.000	13.000	13.000	13.000	13.000	13.000
Number of Edges	66.000	72.000	64.000	39.000	42.000	40.000
Density	0.846	0.923	0.821	0.500	0.538	0.513
Diameter	0.561	1.057	0.684	0.872	1.444	1.019
Transitivity	1.000	0.951	0.971	0.642	0.732	0.761

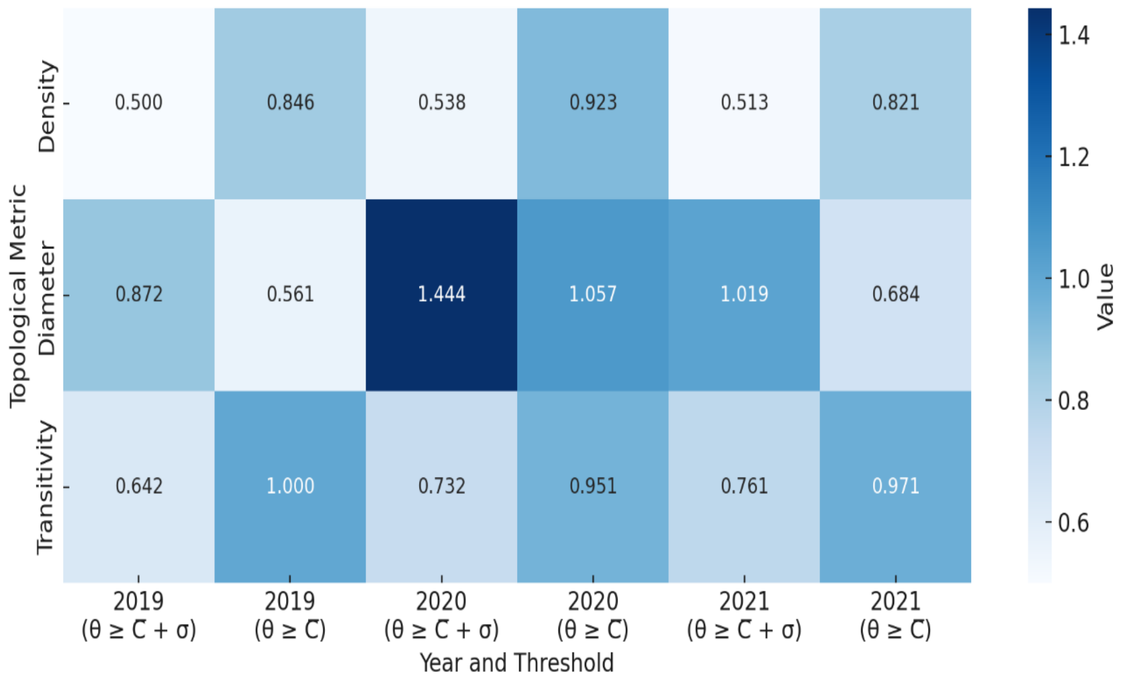

Figure 13: Heatmap of Topological Properties by Threshold and Year

5.0 Conclusion and Future Research

To conclude, this study emphasises the impact of COVID-19 on all 13 Bursa Malaysia sectoral indexes, spanning from January 1, 2019, to December 31, 2021. This study aims to identify any changes in the structure of the Malaysian stock market while also determining influential indexes that prevail throughout the subperiods by utilising a cross-correlation-based threshold network approach and centrality measures. The results show that the indexes tend to be more interconnected with each other, displaying higher correlations in 2020, indicating that the threshold networks experience a slight change in topology. What can be said of this is that the indexes tend to move together, wherein a negative effect on one index can spread to other indexes easily.

By increasing the threshold value, networks appear sparser; however, the position of each index remains relatively constant throughout the years. This can be confirmed by observing how KLRE remains on the peripherals of the 2019 networks and then KLHC replaces its spot in the 2020 and 2021 networks. The centrality measures, on the other hand, are not consistent in identifying key players when using different measures of centrality. Nonetheless, KLCM, KLIP, KLPR and KLCT tend to appear quite a number of times as top scorers, leading us to believe that they dominate the Malaysian stock market during the pandemic. Nevertheless, the study has several limitations. It relies solely on price-based market indices, without incorporating macroeconomic fundamentals such as interest rates, government policy interventions, or sector-specific economic indicators. Additionally, the use of aggregated sectoral indices may obscure important firm-level variations and intra-sectoral dynamics. These constraints limit the scope for causal inference and may affect the generalizability of the findings.

Future research could address these limitations by integrating fundamental economic variables and firm-level financial data to better explain the underlying forces shaping network structures. Applying dynamic or time-evolving network models would allow researchers to capture the temporal evolution of sectoral interdependencies with greater precision. Moreover, future studies could employ sector-level regressions to examine the determinants of network centrality or contagion or explore unsupervised learning techniques to identify latent structures within financial networks. These extensions would offer more comprehensive insights into financial market behaviour during periods of systemic stress and recovery.

Author Contributions Statement: All authors contributed to the study's conception and design. Data collection and analysis were performed by A.A.D & H.B. The first draft of the manuscript was written by A.A.D & H.B, and then all authors commented on previous versions of the manuscript. All authors read and approved the final manuscript.

Funding Statement*:* This research was financially supported by the Ministry of Higher Education Malaysia Fundamental Research Grant Scheme (FRGS-EC/1/2024/STG06/UIAM/03/2).

Informed Consent Statement: Not applicable.

Data Availability Statement: Not applicable.

Conflict of Interest Statement: All authors declare no conflicts of interest in this paper.

References

Amir, U. A. M., Masdi, N. I., Saad, N. M., Yusof, N. M., & Azmi, S. S. (2022). The volatility of ftse bursa malaysia KLCI during the covid-19 pandemic. *International Journal of Academic Research in Business and Social Sciences*, *12*(4).

Aslam, F., Mohmand, Y. T., Ferreira, P., Memon, B. A., Khan, M., & Khan, M. (2020). Network analysis of global stock markets at the beginning of the coronavirus disease (COVID-19) outbreak. *Borsa Istanbul Review*, 20(S1), S49–S61. https://doi.org/10.1016/j.bir.2020.09.003

Bahaludin, H., Mahamood, F. N. A., Abdullah, M. H., Fauzi, M. A., & Omar, M. (2022). The Impact of the COVID-19 Pandemic on the Interconnectedness of Stocks in Bursa Malaysia. *Matematika*, 69-82.

Boginski, V., Butenko, S., & Pardalos, P. M. (2004). Statistical analysis of financial networks. *Computational Statistics & Data Analysis*, 48(2), 431–443. https://doi.org/10.1016/j.csda.2004.02.004

Bonacich, P. (1987). Power and centrality: A family of measures. *American Journal of Sociology*, 92(5), 1170–1182. https://doi.org/10.1086/228631

Chee, K., Chew, S., Izni, N., Ali, A., Tajuddin, N., Aksah, S., & Chin, J. (2024). Pandemic's impact on Bursa Malaysia sectors: A comprehensive study utilising OLSM and ESM. *Journal of Mathematical Sciences and Informatics*, 10(2). https://doi.org/10.46754/jmsi.2024.06.004

Chow, Y., & Tan, Y. (2022). Impact of COVID-19 and government interventions on Bursa Malaysia sectors. *Journal of Chinese Economic and Foreign Trade Studies*, 15(1), 22–37. https://doi.org/10.1108/jcefts-06-2022-0039

Ruiz Estrada, M. A., Park, D., & Lee, M. (2020). The evaluation of the final impact of Wuhan COVID-19 on trade, tourism, transport, and electricity consumption of China. *Tourism, Transport, and Electricity Consumption of China (March 9, 2020)*.

Freeman, L. C. (1977). A set of measures of centrality based on betweenness. *Sociometry*, 40(1), 35–41. https://doi.org/10.2307/3033543

Lee, K. Y.-M., Jais, M., & Chan, C.-W. (2020). Impact of COVID-19: Evidence from Malaysian stock market. *International Journal of Business and Society*, 21(2), 607–628. https://doi.org/10.33736/ijbs.3274.2020

Li, B., & Pi, D. (2018). Analysis of global stock index data during crisis period via complex network approach. *PLOS ONE*, *13(7)*, e0200600. https://doi.org/10.1371/journal.pone.0200600

Li, R., Zhang, R., Zhang, M., & Zhang, T. (2020). Investment analysis and strategy for COVID-19. *Available at SSRN 3563300*. https://doi.org/10.2139/ssrn.3563300

Liew, V. K.-S., Chia, R. C. J., Riaz, S., & Lau, E. (2022). Is there any day-of-the-week effect amid the COVID-19 panic in the Malaysian stock market?. *The Singapore Economic Review*. https://doi.org/10.1142/S021759082250014X

Mantegna, R. N. (1999). Hierarchical structure in financial markets. *The European Physical Journal B*, 11(1), 193–197. https://doi.org/10.1007/s100510050929

New Straits Times (2020). 14-Day Movement Control Order begins nationwide on Wednesday. (2020, March 16). *New Straits Times*. https://www.nst.com.my/news/nation/2020/03/575180/14-day-movement-control-order-begins-nationwide-wednesday

Nobi, A., Maeng, S. E., Ha, G. G., & Lee, J. W. (2014). Effects of global financial crisis on network structure in a local stock market. *Physica A: Statistical Mechanics and Its Applications*, 407, 135–143. https://doi.org/10.1016/j.physa.2014.03.083

Sah, N., & Wong, W. (2021). The impact of MCO on the stock market and moratorium on banking sector's performance in Malaysia: The case of COVID-19. *Labuan Bulletin of International Business and Finance*, 19(2), 35–42. https://doi.org/10.51200/lbibf.v19i2.3318

Sheikh Yahya, S. F. (2020). COVID-19 pandemic: A timeline of key milestones. Astro Awani. https://www.astroawani.com/berita-malaysia/covid19-pandemic-timeline-key-milestones-275454

Silver, N. C., & Dunlap, W. P. (1987). Averaging correlation coefficients: should Fisher's z transformation be used?. *Journal of applied psychology*, *72*(1), 146.

Song, S., Yazi, E., Morni, F., & Janang, J. (2021). COVID-19 and stock returns: Evidence from Malaysia. *International Journal of Banking and Finance*, 16(2), 117–136. https://doi.org/10.32890/ijbf2021.16.2.5

Tashanova, D., Sekerbay, A., Chen, D., Luo, Y., Zhao, S., & Zhang, T. (2020). Investment opportunities and strategies in an era of coronavirus pandemic. *Available at SSRN 3567445*. https://doi.org/10.2139/ssrn.3567445

Tumminello, M., Aste, T., Di Matteo, T., & Mantegna, R. N. (2005). A tool for filtering information in complex systems. *Proceedings of the National Academy of Sciences*, 102(30), 10421–10426. https://doi.org/10.1073/pnas.0500298102

Výrost, T., Lyócsa, Š., & Baumöhl, E. (2015). Granger causality stock market networks: Temporal proximity and preferential attachment. *Physica A: Statistical Mechanics and Its Applications*, 427, 262–276. https://doi.org/10.1016/j.physa.2015.02.017

World Health Organization. (2022). WHO Coronavirus (COVID-19) dashboard. https://covid19.who.int/

Xia, L., You, D., Jiang, X., & Guo, Q. (2018). Comparison between global financial crisis and local stock disaster on top of Chinese stock network. *Physica A: Statistical Mechanics and Its Applications*, 490, 222–230. https://doi.org/10.1016/j.physa.2017.08.005

Zhang, D., Hu, M., & Ji, Q. (2020). Financial markets under the global pandemic of COVID-19. Finance research letters, 36, 101528. https://doi.org/10.1016/j.frl.2020.101528